IOSR Journal of Mechanical and Civil Engineering (IOSR-JMCE)
e-ISSN: 2278-1684,p-ISSN: 2320-334X, Volume 18, Issue 1 Ser. II (Jan. – Feb. 2021), PP 45-55
www.iosrjournals.org

Numerical simulation of two-phase nanofluid flow inside a tube equipped with a vortex generator

Amir haghighatkhah[a1], Milad abdollahi kahriz,
[a]*Master of Mechanical Engineering*

Abstract
In this study, the effect of simultaneous use of vortex generator and nanofluid inside the pipe with the aim of increasing the heat transfer rate has been investigated. There are two single-phase and two-phase methods for modeling nanofluid flow. Due to the fact that in the basic fluid operation, a separate phase and nanoparticles are also a separate phase, so the use of two-phase models for modeling the behavior of this nanoscale is more accurate.
The effects of Peclet number, Reynolds number, nanoparticlesize and nanofluid mean concentration on the distribution of nanoparticles have been evaluated. The valuesof thermal conductivity and viscosity as the main thermo physical properties of nanofluids changedacross different layers of the liquid due to the heterogeneous distribution of concentration. It wasobserved that an increase in the Peclet number caused heterogeneity in the distribution of the properties.The achieved nanoparticle distribution has been implemented for analysis of nanofluid using two-phasemixture model. It was found that the effect of nanofluid concentration on the Nusselt number was morenoticeable in lower Reynolds numbers due to the insignificant effect of flow momentum on heat transfer.

Key word: *Heat transfer, Nanofluid, Heterogeneous concentration, Turbulent flow, Two phase model*

Date of Submission: 14-01-2021 Date of Acceptance: 29-01-2021

I. Introduction

Suspensions containing nanoparticles with dimensions of 1-100 nanometers have many applications in heating and cooling. In the last decade, many studies have examined the properties and effects of nanofluids on improving heat transfer in thermal systems [9-1]. Due to the limitations of heat transfer, researchers have always been looking for ways to improve heat transfer. Therefore, two categories of active and inactive methods have been proposed. In active methods, an external energy source is used to increase the heat transfer rate. The uses of fan or induction magnetic field are examples of this method. Inactive method does not require an external energy source. The use of turbulator, the use of fins and blades, the use of nanofluids and the use of microchannels are among these categories. In this study, the main goal is to increase the heat transfer inside a pipe by using a rotary generator and nanofluid at the same time. Maxwell first proposed in 1873 that by adding solid particles to the base fluid, its thermal conductivity would increase, and this would be accompanied by problems such as increased pressure drop and wear. Nanofluid was the term Choi first used for the multi-phase fluid in which nanoscale particles was present.

Moravejiet al. [12] in 2013 simulated the cooling and pressure drop of SiC and TiO_2 nanofluids in a mini-channel with a thermal well using simulated computational fluid dynamics and the effect of two Reynolds factors and volume fraction on the heat transfer coefficient. The base of their heat wells is 20 × 20 mm and the volume fraction of nanofluids is 0.8, 1.6, 2.4, 3.2 and 4%. The studies were performed for 5 different nanofluidinput velocities. According to their results, the effect of increasing the speed on the heat transfer coefficient is much greater than the effect of increasing the concentration.

Chen et al. [13] performed a numerical simulation of forced heat transfer and the flow properties of copper oxide and aluminum oxide nanofluids in small tubes using mixed and fuzzy two-phase models. They examined both the laminar and turbulent flows and suggested the relationship between nusselt number and the coefficient of friction for these two flows. According to their results, during turbulent flow, the density and deposition of nanoparticles change the roughness of the pipe. The deposition of nanoparticles during the flow process on the wall makes the inner wall feel smoother than the metal wall, thus reducing the roughness of the wall. Since the simulation does not consider the effect of reducing the roughness of the pipe, the numerical values are 22-60% higher than the experimental data. In their simulations, Anne used a multi-phase model, including a mixing model and an Euler model.

* Corresponding author.

Davarnejad and Jamshidzadehh [14] performed dynamic computational modeling of magnesium oxide-water nanofluids in various concentrations in a turbulent lateral tube. They used the k-ε model to model flow turbulence. They also looked at the problem for the volume fraction of 0.625, 0.125, 0.25, 0.5 and 1%, and the range of Reynolds numbers from 3,000 to 19,000. They used three single-phase, mixed, and VOF models to model the nano-fluid, showing that all three models deliver very close results. However, they showed that by increasing the volume fraction of nanoparticles, the two-phase model is more accurate than the other two models. They concluded that as the volume fraction increased, so did the nusselt number and the friction coefficient, but the effect of the friction coefficient on heat transfer was negligible. Sarafraz and Hormozi[15] studied the thermal transfer, pressure drop, and sedimentation of a multi-walled carbon nanotubes Nano scale in a laboratory heat exchanger. The three operating parameters of flow rate (700 <Re <25000), nano-fluid volume concentration (0.5-1.5%) and nano-fluid inlet temperature (50-70 ^{o}C) on the overall heat transfer coefficient and pressure drop were investigated. According to their results, with increasing concentration and flow rate, heat transfer coefficient and pressure drop increase. However, increasing the inlet temperature only slightly increases the heat transfer coefficient. Overall, this nanofluid has a better overall thermal performance than water. For long-term operating conditions, the sedimentation resistance of this nanofluid was measured, which had a nonlinear behavior and the amount of sedimentation was enhanced by increasing the volumetric concentration of the nanofluid. For volume fraction, 0.5% and 1% nusseltnumber increases by approximately 7% and 14%, respectively. When the volume fraction is 1.5%, the nusselt number suddenly increases relative to the volume fraction 0%. They also showed that using multi-walled carbon tube nanoparticles could increase the heat transfer coefficient by up to 68% compared to water fluid. Rao et al. [16] conducted an experimental study of the heat transfer coefficient for nanofluid. They examined the water-aluminum oxide nanofluid with 28 nanometer nanoparticles. They also looked at changes in the properties of nanofluids based on the volume fraction of nanoparticles, the geometry and the size of the nanoparticles. They then examined a shell-and-tube heat exchanger of the opposite flow and single-pass with several tubes under turbulent forced flow conditions. They performed their study for different volume fractions (0.1%; 0.2%; 03% and 0.4%). They showed that the heat transfer coefficient for nanofluid is higher than that of water at the inlet fluid temperature and the same flow rate. Lawrance et al. [17] conducted an experimental study of heat transfer from electronic equipment using graphene nanofluid. They examined the effect of nanofluid mass flow rate, temperature, and volume fraction of nanoparticles on base fluid (0.4% -0.6%) experimentally. They have shown that this cooling method is far more effective than classical methods and can greatly reduce the failure of electronic equipment. In 2019, Murali et al. [18] examined and analyzed heat transfer and pressure drop characteristics for turbulent nanofluid flow of water-iron oxide in a pipe equipped with a trapezoidal plug using the computational fluid dynamics method. Their study was limited to the Reynolds numbers of 2000 to 12000. They showed that for a pipe equipped with a plug-in, the displacement heat transfer rate is about 35.62% higher than a simple pipe, and the rejection of the use of nanofluid as an operating fluid is 78.6% higher than the transfer heat transfer rate.Nakhchi [19] experimentally studied the optimization of geometric parameters on heat transfer and pressure drop of sinusoidal wave channel. He examined the range of Reynolds 1106 to 2530, considered the sinusoidal wavelength ratio in the range of 0.2 to 0.6, the phase shift in the range of 0 to 180 , and the wave number in the range of 5 to 15. He optimized the geometric parameters and made a general correction for the pressure drop and the disproportionate number inside the sinusoidal channel. He found that the maximum heat transfer ratio to the pressure drop for the range ratio was 0.54, the wave number 11 and the phase zero shift, in which case the correction factor was 1.21. Wijayanta et al. [20] investigated the effect of using double-sided ballet plug-ins on increasing heat transfer coefficient and flow characteristics in two-pipe heat exchangers. They looked at parameters such as fin width ratio (0.31, 0.47 and 0.63) on heat transfer and flow characteristics such as Reynolds numbers (5300 to 14500). They showed the highest value of the nusselt number is obtained for the fin ratio of the fin width of 0.63, which is 177% more than the normal tube. In this case, the friction coefficient is 11.6 times that of a normal pipe. In this case, the coefficient of thermal efficiency is 1.15. They showed that the nusselt number, the thermal efficiency coefficient and the friction factor increase with increasing the ratio of each wing. Chamoli et al. [21] investigated the effect of the use of wing-shaped vortex generators on the thermal performance of exchangers. They looked at the flow for Reynolds numbers between 3,500 and 16,000. Also, the geometric parameters of the plugin that have been studied include the ratio of tip to side, which is considered in the range of 0 to 1, and the angle of attack, which is assumed in the range of 30 to 90 degrees. They used a finite volume method and a Simple algorithm to simulate it. The outputs examined by them include the nusselt number, the friction coefficient and the thermal efficiency. They showed that as the angle of attack increased from 30 to 60, the amount of nusselt number and the friction coefficient increased, and as the angle of attack increased from 60 to 90, both decreased. They showed that the maximum thermal efficiency is 2.20, which is obtained when the angle of the tip of the wing is zero and the angle of attack is 30 degrees. The increase in heat transfer for fluid flow passing through the two-pipe exchanger, on both sides of which are fin-shaped plugins, was investigated numerically by Wijayant et al. [22]. Their variables include the Reynolds number and the angle

of attack of the wing. They showed that in this case, the nusselt numberand the coefficient of friction were 3.7 and 10 times larger than the simple tube, respectively.

It is very common to use helical insert and vortex generators to increase heat transfer in different types of heat exchangers [23]. Chamoli et al. [24] investigated the thermal efficiency of a tubular exchanger with a vortex generator. They showed that the non-dimensional nusselt numberor this exchanger was 4.56 times that of the simple tube. Bartwal et al. [25] experimentally investigated the effect of circular rings and metal wire insert on the thermal efficiency of a heat exchanger. They showed that using these plugins could increase thermal efficiency by up to 2.84 times. Spiral wire plugin is one of the most well-known and widely used types of vortex generators, which has a very low manufacturing cost and is very easy to assemble. Their performance has also been shown to disrupt the flow and thus increase the heat transfer rate in a variety of two-pipe heat exchangers and tubular shells [26]. He et al. [27] experimentally investigated the effect of the cross-sectional area of a coil on thermal efficiency and heat transfer rate in heat exchangers. They showed that using this type of plugin could help 5.7% improve the thermal performance of the exchangers. Piriyarungrod et al. [28] used various arrangements of coil wires to increase heat transfer in heat exchangers. Their experimental results showed that using six small coils around a main coil provides the most optimal geometry to increase the efficiency. Khoshvaght-Aliabadiet al. [29] investigated the thermal efficiency coefficient of U-shaped heat exchangers equipped with a spiral wire insert. They showed that using this type of inserts could increase heat transfer by up to 67% over a simple pipe. Hasanpour et al. [30] experimentally and numerically examined heat transfer and pressure drop in tube shell exchangers equipped with a variety of spiral wire inserts. They found that the thermal efficiency coefficient is often more than one unit, with a maximum value of 1.5, which is obtained for the V-shaped insert. Abed et al. [31] conducted a numerical study of heat transfer in a heat exchanger with a V-shaped spiral wire insert. They showed that if the torsion factor was 4 and the Reynolds number was 9000, using the V-shaped plugin could increase the nusselt number value by 8.75 times. Rashidi et al. [32] numerically examined the heat transfer of turbulent flow in a tube equipped with a helical insert. They were studied in the range of Reynolds numbers from 5,000 to 12,000. They reported that the use of the spiral plug-in output from center 3.5 shows the highest thermal efficiency and can increase the heat transfer rate by up to 33%.Rahimiet al. [33] investigated the thermal and hydraulic efficiency of pipes equipped with different types of inserts. They examined the issue numerically and experimentally. They showed that the maximum increase in heat transfer rate when using these inserts is 31%.

Nakhchi and Esfahani [34] investigated the thermal efficiency of turbulent fluid flow inside a tube heat exchanger using a V-shaped insert. They looked at the ratio of different cuts (0.6 to 1.8), Reynolds numbers ranging from 5,000 to 15,000. They used the computational fluid dynamics method to numerically simulate. They used the $k-\varepsilon$model to model turbulent flow. They also compared numerical values with experimental data to validate the developed model. It showed that for the coefficients of 0.6, 1, 1.4 and 1.8, the rate of increase in heat transfer is 48%, 64.3%, 86% and 117.4%, respectively. They also showed that the maximum thermal efficiency coefficient is 1.83, which is obtained for the shape ratio of 1.8 and the Reynolds number 5000.Ahmed et al. [35] performed a three-dimensional numerical simulation of the heat transfer of nanoparticles of water-copper oxide and water-aluminum oxide in a triangular duct with a vortex generator. They examined the effect of nanofluid type and volume fraction. Because it has a triangular channel, low pressure drop, and low heat transfer coefficient compared to other channels, two inactive nanofluid methods and a vortex generator have been used to help increase heat transfer.According to their results, the heat transfer rate in the triangular channel with the blade and using nanofluid is higher than the bladeless channel. The increase in heat transfer due to the alumina-water nanofluid is greater than that of the copper oxide-water,which is due to the larger alumina parenteral number. Also, an increase in the nanofluid concentration increases the effective thermal conductivity of the nanofluid, which leads to an increase in heat transfer from the hot wall to the cold fluid. The increase in viscosity is greater than the increase in the thermal conductivity of the nanofluid and therefore the increase in the number of prandtl number. Ali Akbari[36] examined the effect of bulk nanoparticle fraction as well as the shape coefficient of the coil wire insert for the flow of aluminum oxide-water nanofluid for Reynolds numbers in the range of 500 to 25000 numerically and using computational fluid dynamics. They showed that as the volume fraction of nanoparticles in the base fluid increased, the heat transfer rate increased. Ramanathan [37] analyzed the efficiency of spiral insert in a two-pipe heat exchanger using water-aluminum oxide nanofluid. They showed that the heat transfer coefficient increased by about 7.5% compared to the base state. Eiamsaet al. [38] investigated the increase in water-silver nanofluid heat transfer inside a tube equipped with a micro fin and non-homogeneous spiral wire inserts. They examined the effect of reducing the twisting coefficient and increasing the concentration of nanoparticles in the base fluid on heat transfer rate, pressure drop, friction losses and increasing the efficiency factor. Maddah and Aghayari [39] used hybrid nanofluid aluminum oxide-titanium oxide-water in a shell and tube heat exchanger to test the increase in thermal efficiency experimentally. They studied the random motions and scattering of nanoparticles, which intensified the momentum exchange rate between nanoparticles, especially near the walls, and thus increased the axial pressure drop of the current.

Kumar and Singh [40] conducted an experimental study of the hydrodynamic and thermal efficiency of a heat exchanger with spherical disk inserts. They looked at the constant diameter ratio of 0.8, the torsion ratio of 1, 2, and 3, and the fixed rotation ratio of 2 for Reynolds numbers 6500 to 26500. They showed that this could improve the heat transfer rate by 2.2 to 3.54 times and the efficiency by 1.18 to 1.64 times that of conventional exchangers. Shi et al. [41] examined the effect of geometric parameters and Reynolds number on heat transfer and the characteristics of rectangular micro channel flow using nanofluid as the operating fluid. They examined the nanofluid flow of water-aluminum oxide for the Reynolds range of laminar flows. They showed that with increasing the coefficient of shape, the amount of local nusselt numberalso increases. It should be noted that in their study, the hydraulic diameter of 0.12 mm and the volume fraction of nano particles in base fluid 1% and nanoparticle diameter constant and equal to 40 Nanometers were considered, and Reynolds numbers ranged from 9.7 to 2000 (laminar flow). They also showed that the average nusselt number for microchannels for all shape ratio and design variables in the range of Reynolds numbers examined was higher than normal channels. However, with increasing Reynolds numbers and decreasing the shape ratio, the difference between the microchannel and normal channels becomes more noticeable. They also showed that for a fixed Reynolds number, the amount of friction coefficient increases with increasing shape factor.Gnanavel et al. [42] investigated the increase in heat transfer through the nanofluidand spiral insert with rectangular cuts in the heat exchanger. They used copper oxide nanoparticles, titanium oxide, zinc oxide and beryllium oxide with water-based fluid as the operating fluid.Hemmat et al. [43] studied the three-dimensional numerical natural heat transfer of nanofluid flow inside a cubic cavity equipped with porous fins . They used a two-phase mixed model to model the nanofluid. They considered the volume fraction of nanofluid in the range of 0% to 3% and considered 1, 2 and 3 blades in cavity. They showed that heat transfer improves with increasing volume fraction and Reynolds number. Although the two-phase model increases computational costs over the single-phase model, they do increase the accuracy of numerical calculations. Ma et al. [44] simulated two-phase nanofluid flow and examined the effect of blade arrangement on the first and second laws efficiency for water-silver nanofluids. They measured the effect of parameters such as volume fraction of nanoparticles, Reynolds number on displacement heat transfer coefficient, surface temperature, pump required power, heat transfer and friction coefficient. They showed that the best value was obtained for the return of the first and second laws of the volume fraction of 0.1% and Reynolds 500 and the linear arrangement of the blades. Rajabi et al. [45] examined the numerical simulation of the turbulent nanofluid flow in a narrow channel with a wall that was heated. They used a single-phase model and a two-phase model to model the nanofluid flow. They studied volumetric fractions of 0, 2%, and 4%, and examined the pressure coefficient, friction coefficient, heat transfer coefficient, and different contours for different states. They showed that as the cavity depth increases, the pressure coefficient becomes more negative.

II. Governing equations

In order to analyze the flow behavior for all flows, the equations for mass conservation and momentum are solved. For compressible flows or flows including heat transfer, energy equations are also solved. Turbulent modeling equations should be used when the flow is turbulent. The purpose of modeling turbulent flows is to determine terms such as Reynolds stress, turbulent mass flux, or turbulent thermal flux.

Continuity equation

$$\frac{1}{r}\frac{\partial(rv)}{\partial r}+\frac{\partial u}{\partial x}=0 \quad (1)$$

Momentum equation in the x direction

$$\rho_{nf}\left[u\frac{\partial u}{\partial x}+v\frac{\partial u}{\partial r}\right]=-\frac{\partial p}{\partial x}+\mu_{nf}\left[\frac{1}{r}\frac{\partial}{\partial r}\left(r\frac{\partial u}{\partial r}\right)+\frac{\partial^2 u}{\partial x^2}\right] \quad (2)$$

Momentum equation in the r direction

$$\rho_{nf}\left[u\frac{\partial v}{\partial x}+v\frac{\partial v}{\partial r}\right]=-\frac{\partial p}{\partial r}+\mu_{nf}\left[\frac{\partial}{\partial r}\left(\frac{1}{r}\frac{\partial}{\partial r}(rv)\right)+\frac{\partial^2 v}{\partial x^2}\right] \quad (3)$$

Energy equation

$$\left(\rho C_p\right)_{nf}\left[\frac{\partial(uT)}{\partial x}+\frac{1}{r}\frac{\partial(rvT)}{\partial r}\right]=k_{nf}\left[\frac{\partial^2 T}{\partial x^2}+\frac{1}{r}\frac{\partial}{\partial r}\left(r\frac{\partial T}{\partial r}\right)\right] \quad (4)$$

By defining the dimensionless variables

$$u^*=\frac{u}{u_c},\ v^*=\frac{v}{u_c},\ R^*=\frac{r}{R},\quad x^*=\frac{x}{R\,Re\,Pr},\ P^*=\frac{p}{\rho_{nf}u_c^2},\quad Pr=\frac{(\mu C_p)_f}{k_f},\quad Re=\frac{\rho_f u_c D}{\mu_f},\quad \theta=\frac{T-T_c}{T_{h1}-T_c} \quad (5)$$

In the above relations, u_c indicates the fluid velocity at the inlet of the pipe, R is the radius of the pipe and D is the diameter of the pipe, which is twice the radius. T_c is the temperature of the input nanofluid and T_{h1} is the temperature of the hot wall of the pipe. By applying the introduced dimensionless parameters, the dimensionless equations are obtained as follows:

Dimensionless momentum equation in the direction of x

$$\frac{\partial}{\partial x^*}\left[u^*u^* - \left(\frac{\mu_{nf}}{\mu_f}\frac{\rho_f}{\rho_{nf}}\frac{2}{Re^2 Pr}\frac{\partial u^*}{\partial x^*}\right)\right] + Re.Pr\frac{1}{R^*}\frac{\partial}{\partial R^*}\left[R^*\left(u^*v^* - \left(\frac{\mu_{nf}}{\mu_f}\frac{\rho_f}{\rho_{nf}}\frac{2}{Re}\frac{\partial u^*}{\partial R^*}\right)\right)\right] = -\frac{\partial P^*}{\partial x^*}(6)$$

Dimensionless momentum equation in the direction of r

$$\frac{1}{Re.Pr}\frac{\partial}{\partial x^*}\left[u^*v^* - \left(\frac{\mu_{nf}}{\mu_f}\frac{\rho_f}{\rho_{nf}}\frac{2}{Re^2 Pr}\frac{\partial v^*}{\partial x^*}\right)\right] + \frac{1}{R^*}\frac{\partial}{\partial R^*}\left[R^*\left(v^*v^* - \left(\frac{\mu_{nf}}{\mu_f}\frac{\rho_f}{\rho_{nf}}\frac{2}{Re}\frac{\partial v^*}{\partial R^*}\right)\right)\right] = -\frac{\partial P^*}{\partial R^*} - \frac{\mu_{nf}}{\mu_f}\frac{\rho_f}{\rho_{nf}}\frac{2}{Re}\frac{v^*}{R^{*2}}(7)$$

Dimensionless energy equation

$$\frac{\partial y}{\partial x^*}\left[u^*\theta - \left(\alpha_{nf}\frac{\rho_f}{\mu_f}\frac{2}{Re.Pr}\frac{\partial\theta}{\partial x^*}\right)\right] + Re.\Pr\frac{1}{R^*}\frac{\partial}{\partial R^*}\left[R^*\left(v^*\theta - \left(\alpha_{nf}\frac{\rho_f}{\mu_f}\frac{2}{Re}\frac{\partial\theta}{\partial R^*}\right)\right)\right] = 0(8)$$

The $k-\varepsilon$model is used to simulate flow turbulence. The $k-\varepsilon$model is expressed on the concept of vortex viscosity and$\mu_{ref} = \mu + \mu_t$. In this model, it is assumed that $\mu_t$depends on the kinetic energy of the flow and the decrease in energy according to the following relation.

$$\mu_t = C_\mu \rho\frac{k^2}{\varepsilon} \quad (9)$$

$C_\mu$isa fixed number. The values of k and ε are obtained directly from the differential equations of kinetic energy transfer and the rate of turbulent energy loss as follows:

$$\frac{\partial \rho k}{\partial t} + \frac{\partial}{\partial x_j}(\rho u_j k) = \frac{\partial}{\partial x_j}\left[\left(\mu + \frac{\mu_t}{\sigma_k}\right)\frac{\partial k}{\partial x_j}\right] + P_k - \rho\varepsilon + P_{kb}(10)$$

$$\frac{\partial \rho\varepsilon}{\partial t} + \frac{\partial}{\partial x_j}(\rho u_j \varepsilon) = \frac{\partial}{\partial x_j}\left[\left(\mu + \frac{\mu_t}{\sigma_\varepsilon}\right)\frac{\partial \varepsilon}{\partial x_j}\right] + \frac{\varepsilon}{k}(C_{\varepsilon 1}P_k - C_{\varepsilon 2}\rho\varepsilon + C_{\varepsilon 1}P_{\varepsilon b}$$

$C_{\varepsilon 1}$ ،$C_{\varepsilon 2}$ ،$\sigma_k$and $\sigma_\varepsilon$are fixed. $P_{kb}$and $P_{\varepsilon b}$express the effect of buoyance forces. P_k is the production of turbulence due to viscous forces.

$$P_k = \mu_t\left(\frac{\partial u_j}{\partial x_j} + \frac{\partial u_i}{\partial x_i}\right)\frac{\partial u_i}{\partial x_j} - \frac{2}{3}\frac{\partial u_k}{\partial x_k}(3\mu_t\frac{\partial u_k}{\partial x_k} + \rho k)(11)$$

III. Euler-Lagrange two-phase method

In this method, the presence and distribution of particles in the base fluid are considered separately. Thus, the conservation equations are written for the continuous phase, and the effects of the presence and distribution of nanoparticles in the base fluid are considered as source terms in the momentum and energy equations. This method, as its name implies, follows Euler's and Lagrange's theory. The liquid phase acts as a continuous phase, the specifications of which are determined by solving the equations of navier stokes equation, while the characteristics of the distributed phase are determined by examining a large number of particles in the flow field and considering Newton's second law for each particle. The diffused phase can exchange momentum, mass, and energy with the liquid phase. For the liquid phase, the conservation equations are as follows:

Continuity

$$\nabla.(\rho_f\vec{v}_f) = 0(12)$$

$$\nabla.(\rho_f\vec{v}_f\vec{v}_f) = -\nabla P + \nabla.(\mu_f\nabla\vec{v}_f) + \rho_f\vec{g}\beta(T - T_i) + \vec{S}_m(13)$$

In the above relationship, the S_m is source term represents the momentum transferred between the fluid phase and the particle phase, which is determined by calculating the change in the momentum of the particles passing through the control volume.

$$\vec{S}_m = \sum\vec{F}m_p\Delta t(14)$$

The m_p is the particle mass and $\vec{F}$indicate the sum of all the forces on the unit of mass of the nanoparticle that is applied to the particle, including the drag force that we show with $\vec{F}_D$, the gravitational force that we show with $\vec{F}_G$, the force of virtual mass we show it with $\vec{F}_V$, theSaffmanlift force we show it with $\vec{F}_L$, the thermophoretic force we show it with $\vec{F}_T$, the Brownian force we show it with $\vec{F}_B$, and finally the pressure gradient force that it We show $\vec{F}_P$, which is given in the following for the computational relationships of each.

It should be noted that for nanoparticles, the equation for particle motion can be expressed according to Newton's second law as follows:

$$F = \frac{d\vec{v}_p}{dt}(15)$$

For lower micron particles, due to the small relative Reynolds number, the drag force is determined by the following using the Stokes rule:

$$\vec{F}_D = \frac{18\mu}{d_p^2\rho_p C_e}(\vec{v}_f - \vec{v}_p)(16)$$

$$C_e = 1 + \frac{2\lambda}{d_p}(1.257 + 0.4e^{-\left(\frac{1.1d_p}{2\lambda}\right)})(17)$$

In the above relationλ is the average the free path molecular.

The lift force on a particle is caused by the rotation of the velocity gradient and can be calculated from the following relation:

$$\vec{F}_L = \frac{2Kv^{\frac{1}{2}}\rho d_{ij}}{\rho_p d_p (d_{lk} d_{kl})^{\frac{1}{4}}} (\vec{v}_f - \vec{v}_p) (18)$$

That $k = 2.594$ and $d_{ij}$are deformed tensors. This form of lift force has meaning for tiny particles.

It should be noted that this relationship can be used for micron particles.

Another force applied to small particles in the fluid is the Brownian force. For the particles under the micron, the collision of the particles with the fluid molecules and therefore the effect of the Brownian motion become important. The components of the Brownian force are modeled by the Gaussian disturbance process with the intensity of the $S_{n.ij}$ spectrum, according to which we have:

$$S_{ij}^n = S_0 \delta_{ij} (19)$$

Which is in the above relationsδ_{ij} is Kronecker deltaand

$$S_0 = \frac{216 v k_B T}{\pi^2 \rho_f d^S (\frac{\rho_p}{\rho_f})^2 C_e} (20)$$

In the above relation, T is the absolute fluid temperature and v is the kinematic viscosity and k_B is the Boltzmannconstant. The magnitude of the components of the Brownian force is as follows:

$$\vec{F}_{B.i} = \xi_i \sqrt{\frac{\pi S_0}{\Delta t}} (21)$$

In the above relationξ_i is the random Gauss numbers with independent single varianceand the mean of zero.

Another force applied to small particles in the fluid is the thermophoretic force. This force is calculated by the following equation:

$$\vec{F}_T = -D_{T.p} \frac{1}{m_P T} \nabla . T (22)$$

In the above relation, $D_{T.P}$is the thermo physicalcoefficient which can be calculated from the following relation:

$$D_{T.p} = \frac{6\pi d_p \mu_f^2 C_s (\frac{k_f}{k_p} + 2C_t Kn)}{\rho_f (1 + 6C_m Kn)(1 + 2\frac{k_f}{k_p} + 4C_t Kn)} (23)$$

The above relation is known as the Talbot relation, in which $C_m = 2.28$, $C_s = 1.17$, and $C_t = 4.36$, which are called the momentum exchange coefficient, thermal slip coefficient, and thermal jump coefficient, respectively. Kn is Knudsen number that is defined as follows:

$$Kn = \frac{2\lambda}{d_P} (24)$$

The force of the virtual mass required to accelerate the fluid around the particle is expressed as follows:

$$\vec{F}_v = \frac{1}{2} \frac{\rho_f}{\rho_p} \frac{d}{dt} (\vec{v}_f - \vec{v}_p) (25)$$

The gravitational force and pressure gradient are also calculated by the relations (26) and (27), respectively:

$$F_G = \frac{\vec{g}(\rho_p - \rho_f)}{\rho_p} (26)$$

$$\vec{F}_p = \left(\frac{\rho_f}{\rho_p}\right) \vec{v}_p . \nabla v_f (27)$$

The energy equation is also written as follows:

$$\nabla . \left(\rho_f c_{p.f} \vec{v}_f T_f\right) = \nabla . (k_f \nabla T_f) + S_e (28)$$

In the above relation, the $S_e$term indicates the warm wall term due to the exchange of thermal energy of the particle and the fluid and is expressed as follows:

$$S_e = \sum \dot{Q} \Delta t (29)$$

In the above relation $\dot{Q}$ is the total heat flux rate exchanged between the particle and the fluid, which is calculated by the following relation:

$$\dot{Q} = Nu \, \pi \, d_p k_f (T_p - T_f) (30)$$

In the above relation, Nu represents the dimensionless Nusselt number, which is calculated using the Ranz and Marshall equations, the following is calculated:

$$Nu = 2 + 0.6 Re_d^{\frac{1}{2}} Pr^{\frac{1}{3}} (31)$$

IV. Numerical method and validation

Finite volume method has been used to solve the governing equations in this study. Also, the second order method has been used to discrete the momentum and energy equations, and the equations of the velocity and pressure vectors have been solved as a coupling, and the SIMPLE algorithm has been used. In order to better understand the gradients of velocity and temperature in the wall of the pipe where the boundary layer is

formed, finer meshing is used in these areas. It is assumed that there is a constant heat on the wall of the flux tube. The nanofluid velocity at the inlet of the pipe is uniform and its temperature is considered to be 300°K. Nanofluid is a water-Fe_2O_3used. A free jet condition is used at the outlet of the pipe. There is a non-slip condition for all walls. A view of the geometry of the pipe with its vortex generator can be seen in Figure (1).

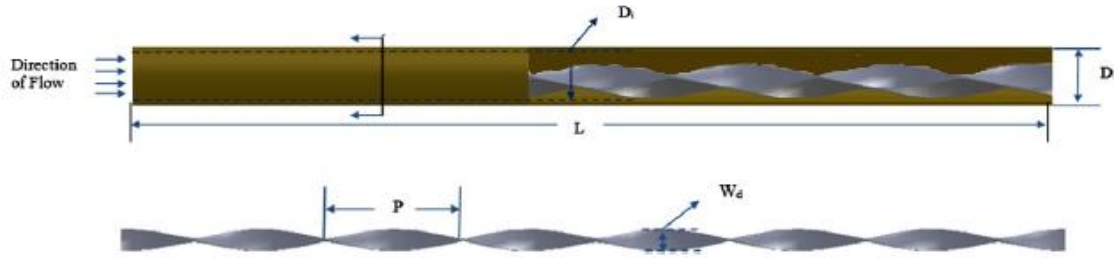

Figure1. Schematic of geometry

For different meshes, the independence of the grid has been investigated and its results are shown in Figure (2).

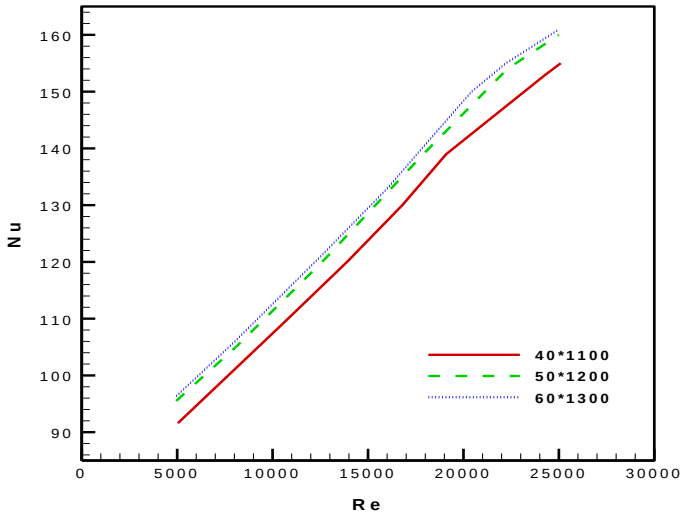

Fig2. Grid independency results

According to the results presented in Figure (2), 1200 x 50 mesh has been used as the optimal state in this study. Also for the validation of the developed numerical model, the results obtained with the experimental data provided by Sundar et al. [46] compare. The results are shown in Figure (3).

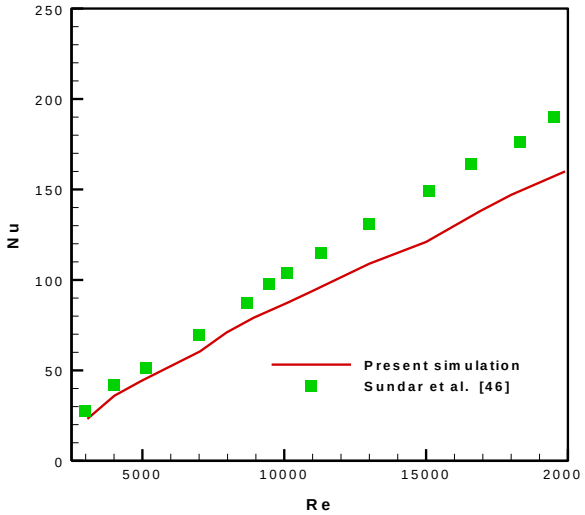

Figure3. Numerical model validation developed

According to Figure (3), it can be seen that the developed numerical model has sufficient accuracy.

V. Results

Figure (4) shows the distribution of nanoparticles at the cross-sectional area of the pipe and for the average volume fraction of 1% and 4% per different numbers of peclet number (Pe). It is observed that as the peclet numberincreases, the amount of heterogeneity of nanoparticle distribution increases.

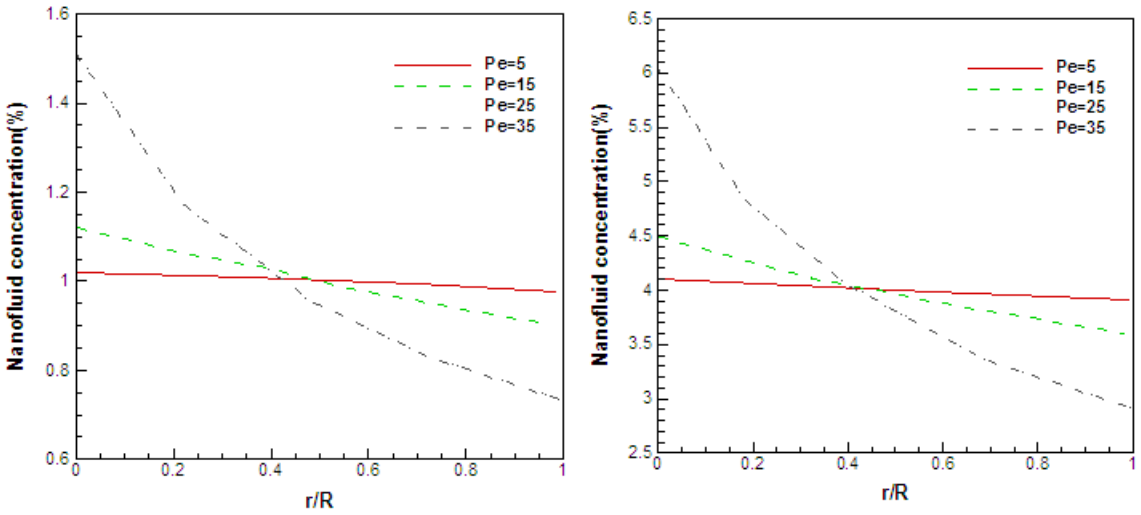

Figure4. Nanofluid concentration distribution at various Peclet numbers for mean concentration of (left) 1% and (right) 4%.

For example, for Pe = 35, the concentration of the particle increases from 2.92% near the wall to 6.07% in the center for a 4% volume fraction. In fact, as the number of Peclet increases, so does the share of Brownian movements relative to other factors. In other words, the effect of Brownian motions on the Peclet number is greater, and as a result the distribution of nanoparticle concentration is more uniform. Therefore, for Pe = 5 and a large fraction of 4%, the concentration of nanoparticles increases from 3.90% near wall to 4.10% in the center of the tube.

Figure 5 shows the distribution of nanoparticle concentration at the pipe cross-section for different values of Reynolds number in 1% and 4% volume fraction and 40 nm nanoparticle diameters.

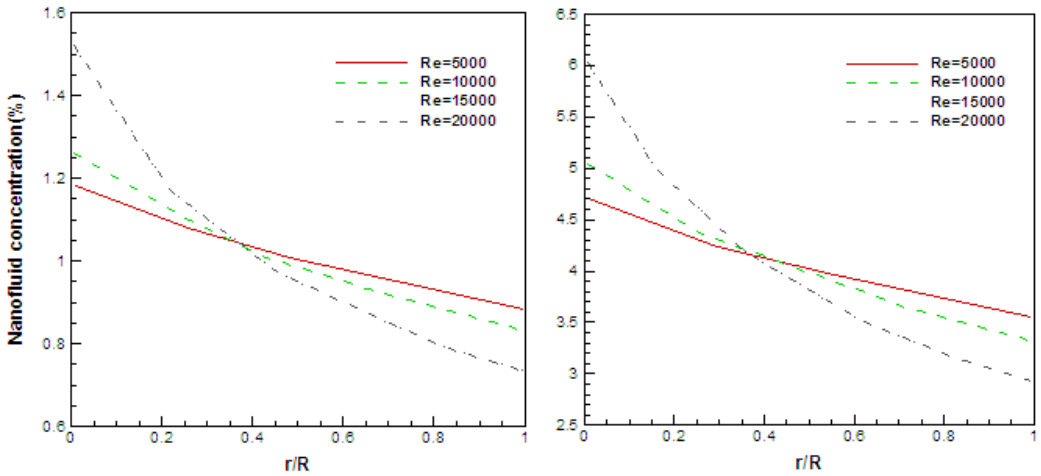

Figure5. Nanofluid concentration distribution at various Reynolds numbers for mean concentration of (left) 1% and (right) 4%.

It is seen thatthe increment of Reynolds number leads to non-uniform concentrationdistribution. With incrementing Reynolds numbers the pressuregradient increases in the nanofluid and the Peclet number raises. Therefore, the effect of shear rate is morepronounced compared to Brownian motion in high Reynolds numbersand causes spatial heterogeneity in concentrationdistribution.

Figures (6) and (7) for Reynolds numbers and different volume fractions show the changes in the nusselt numberand the friction coefficient, respectively.

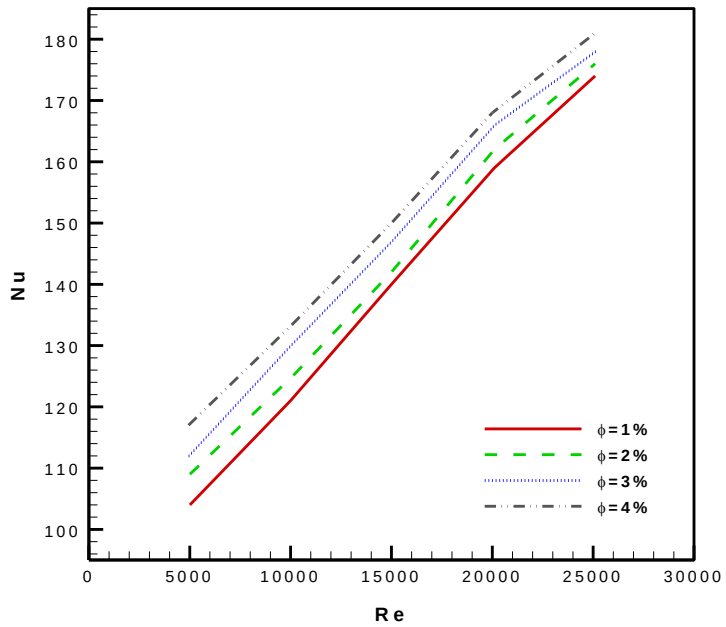

Figure6. Nusselt number versus Reynolds number for different mean concentrations

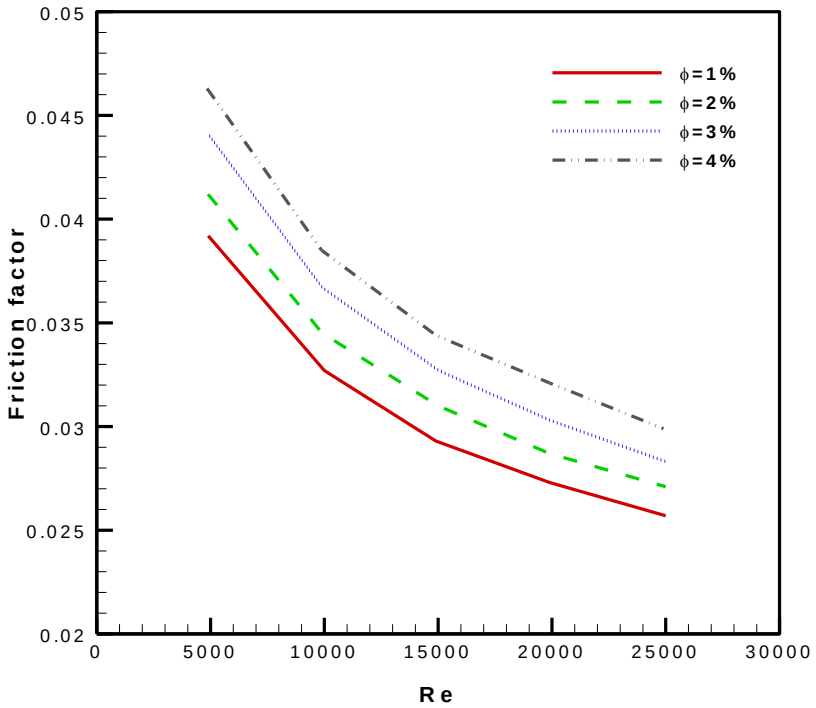

Figure6. Friction factor versus Reynolds number for different mean concentrations

VI. Conclusion

A numerical analysis was conducted to evaluate flow and heattransfer of Fe_2O_4 -water nanofluids in a tube with vortex generator for turbulentregime considering heterogeneous concentration distribution

using two-phase mixture model. The concentration distributionheterogeneity enhances with theincrement of Reynolds number,Peclet number, nanoparticle size and means concentrations. Thisspatial heterogeneity leads to non-uniform thermo physical properties.The higher thermal conductivity near the tube surface wasachieved due to the higher concentration of the particles in thatregion. The achieved nanoparticle distribution was implementedfor analysis of nanofluid using two-phase mixture model. It wasobserved that incrementing Reynolds number and nanofluid meanconcentration lead to the Nusselt number enhancement. The influenceof nanofluid concentration on the Nusselt number was morenoticeable in lower Reynolds numbers due to the insignificantinfluence of flow momentum on heat transfer. The maximum of43.9% enhancement in

convection heat transfer was reached by dispersion of 4% Fe_3O_4nanoparticles inside water at Re = 25,000. Itwas observed that the friction factor decreased with the incrementof Reynolds number and nanoparticle mean concentration. Thethermal performance index of the Fe_3O_4 -water nanofluid wasattained greater than unity in all conditions. Therefore, heat transferimprovement overcomes the increment of friction factor in thepresent work. Moreover, it was revealed that the results of numericalanalysis considering heterogeneousconcentration distributionwere in reasonable agreement with the experimental data, whilethe experimental data were overrated by considering homogeneousconcentration distribution.

References

[1]. Amani, Mohammad, Mohammad Ameri, and Alibakhsh Kasaeian. "The efficacy of magnetic field on the thermal behavior of MnFe2O4 nanofluid as a functional fluid through an open-cell metal foam tube." *Journal of Magnetism and Magnetic Materials* 432 (2017): 539-547.

[2]. Milanese, M., et al. "Optical absorption measurements of oxide nanoparticles for application as nanofluid in direct absorption solar power systems–Part I: water-based nanofluids behavior." *Solar Energy Materials and Solar Cells* 147 (2016): 315-320.

[3]. Milanese, M., et al. "Optical absorption measurements of oxide nanoparticles for application as nanofluid in direct absorption solar power systems–Part II: ZnO, CeO2, Fe2O3 nanoparticles behavior." *Solar Energy Materials and Solar Cells* 147 (2016): 321-326.

[4]. Milanese, Marco, et al. "An investigation of layering phenomenon at the liquid–solid interface in Cu and CuO based nanofluids." *International Journal of Heat and Mass Transfer* 103 (2016): 564-571.

[5]. Amani, Mohammad, Mohammad Ameri, and Alibakhsh Kasaeian. "Investigating the convection heat transfer of Fe3O4 nanofluid in a porous metal foam tube under constant magnetic field." *Experimental Thermal and Fluid Science* 82 (2017): 439-449.

[6]. Amani, Mohammad, Mohammad Ameri, and Alibakhsh Kasaeian. "The experimental study of convection heat transfer characteristics and pressure drop of magnetite nanofluid in a porous metal foam tube." *Transport in Porous Media* 116.2 (2017): 959-974.

[7]. Colangelo, Gianpiero, and Marco Milanese. "Numerical simulation of thermal efficiency of an innovative Al2O3 nanofluid solar thermal collector: Influence of nanoparticles concentration." *Thermal Science* 21.6 Part B (2017): 2769-2779.

[8]. Colangelo, Gianpiero, et al. "Thermal conductivity, viscosity and stability of Al2O3-diathermic oil nanofluids for solar energy systems." *Energy* 95 (2016): 124-136.

[9]. Colangelo, Gianpiero, et al. "Experimental test of an innovative high concentration nanofluid solar collector." *Applied Energy* 154 (2015): 874-881.

[10]. Maxwell, James Clerk. *A treatise on electricity and magnetism*. Vol. 1. Clarendon press, 1881.

[11]. Choi, Stephen US, and Jeffrey A. Eastman. *Enhancing thermal conductivity of fluids with nanoparticles*. No. ANL/MSD/CP-84938; CONF-951135-29. Argonne National Lab., IL (United States), 1995.

[12]. Moraveji, Mostafa Keshavarz, Reza Mohammadi Ardehali, and Ali Ijam. "CFD investigation of nanofluid effects (cooling performance and pressure drop) in mini-channel heat sink." *International Communications in Heat and Mass Transfer* 40 (2013): 58-66.

[13]. Chen, Yan-jun, Yuan-yang Li, and Zhen-hua Liu. "Numerical simulations of forced convection heat transfer and flow characteristics of nanofluids in small tubes using two-phase models." *International Journal of Heat and Mass Transfer* 78 (2014): 993-1003.

[14]. Davarnejad, Reza, and Maryam Jamshidzadeh. "CFD modeling of heat transfer performance of MgO-water nanofluid under turbulent flow." *Engineering Science and Technology, an International Journal* 18.4 (2015): 536-542.

[15]. Sarafraz, M. M., and F. Hormozi. "Heat transfer, pressure drop and fouling studies of multi-walled carbon nanotube nano-fluids inside a plate heat exchanger." *Experimental Thermal and Fluid Science* 72 (2016): 1-11.

[16]. Rao, M. Siva Eswara, et al. "Experimental investigation on forced convective heat transfer coefficient of a nano fluid." *Materials Today: Proceedings* 4.8 (2017): 8717-8723.

[17]. Lawrance, LK Babith, and R. Rohith Renish. "Experimental investigation of heat transfer from an electronic device using graphene nano fluid." *Materials Today: Proceedings* 5.9 (2018): 20669-20678.

[18]. Murali, G., B. Nagendra, and J. Jaya. "CFD analysis on heat transfer and pressure drop characteristics of turbulent flow in a tube fitted with trapezoidal-cut twisted tape insert using Fe3O4 nano fluid." *Materials Today: Proceedings* (2019).

[19]. Nakhchi, Mahdi E. "Experimental optimization of geometrical parameters on heat transfer and pressure drop inside sinusoidal wavy channels." *Thermal Science and Engineering Progress* 9 (2019): 121-131.

[20]. Wijayanta, Agung Tri, et al. "Double-sided delta-wing tape inserts to enhance convective heat transfer and fluid flow characteristics of a double-pipe heat exchanger." *Applied Thermal Engineering* 145 (2018): 27-37.

[21]. Chamoli, Sunil, et al. "Thermal performance improvement of a solar air heater fitted with winglet vortex generators." *Solar Energy* 159 (2018): 966-983.

[22]. Wijayanta, Agung Tri, et al. "Numerical study of heat transfer enhancement of internal flow using double-sided delta-winglet tape insert." *Energies* 11.11 (2018): 3170.

[23]. Chamoli, Sunil, Peng Yu, and Shimin Yu. "Multi-objective shape optimization of a heat exchanger tube fitted with compound inserts." *Applied Thermal Engineering* 117 (2017): 708-724.

[24]. Chamoli, Sunil, et al. "Numerical study on flow structure and heat transfer in a circular tube integrated with novel anchor shaped inserts." *Applied Thermal Engineering* 135 (2018): 304-324.

[25]. Bartwal, Amit, et al. "Thermal performance intensification of a circular heat exchanger tube integrated with compound circular ring–metal wire net inserts." *Chemical Engineering and Processing-Process Intensification* 124 (2018): 50-70.

[26]. Nakhchi, Mahdi Erfanian, and J. A. Esfahani. "Sensitivity analysis of a heat exchanger tube fitted with cross-cut twisted tape with alternate axis." *Journal of Heat Transfer* 141.4 (2019).

[27]. He, Yan, et al. "Experimental study on heat transfer enhancement characteristics of tube with cross hollow twisted tape inserts." *Applied Thermal Engineering* 131 (2018): 743-749.

[28]. Piriyarungrod, N., et al. "Intensification of thermo-hydraulic performance in heat exchanger tube inserted with multiple twisted-tapes." *Applied Thermal Engineering* 136 (2018): 516-530.

[29]. Khoshvaght-Aliabadi, M., S. Davoudi, and M. H. Dibaei. "Performance of agitated-vessel U tube heat exchanger using spiky twisted tapes and water based metallic nanofluids." *Chemical Engineering Research and Design* 133 (2018): 26-39.

[30]. Hasanpour, A., M. Farhadi, and K. Sedighi. "Intensification of heat exchangers performance by modified and optimized twisted tapes." *Chemical Engineering and Processing-Process Intensification* 120 (2017): 276-285.

[31]. Abed, Azher M., et al. "Numerical analysis of flow and heat transfer enhancement in a horizontal pipe with P-TT and V-Cut twisted tape." *Case studies in thermal engineering* 12 (2018): 749-758.
[32]. Rashidi, Saman, N. Moghadas Zade, and J. Abolfazli Esfahani. "Thermo-fluid performance and entropy generation analysis for a new eccentric helical screw tape insert in a 3D tube." *Chemical Engineering and Processing: Process Intensification* 117 (2017): 27-37.
[33]. Rahimi, Masoud, Sayed Reza Shabanian, and Ammar Abdulaziz Alsairafi. "Experimental and CFD studies on heat transfer and friction factor characteristics of a tube equipped with modified twisted tape inserts." *Chemical Engineering and Processing: Process Intensification* 48.3 (2009): 762-770.
[34]. Nakhchi, M. E., and J. A. Esfahani. "Performance intensification of turbulent flow through heat exchanger tube using double V-cut twisted tape inserts." *Chemical Engineering and Processing-Process Intensification* 141 (2019): 107533.
[35]. Ahmed, Hamdi E., et al. "Turbulent heat transfer and nanofluid flow in a triangular duct with vortex generators." *International Journal of Heat and Mass Transfer* 105 (2017): 495-504.
[36]. Omid Ali Akbari, Investigation of the volume fraction of nanoparticles effect and aspect ratio of the twisted tape in the tube, Thermal Anal calorie 129 (2017) 1911–1922.
[37]. Ramanathan, Performance analysis on the double pipe heat exchanger with twisted tape inserts using Al2O3-Water based Nanofluid, Int. J. Automot. Technol. (2018).
[38]. Smith Eiamsa-ard, Khwanchit Wongcharee, Convective heat transfer enhancement using Ag-water Nanofluid in a micro-fin tube combined with non-uniform twisted tape, Int. J. Mech. Sci. (2018).
[39]. Heydar Maddah, Reza Aghayari, Factorial experimental design for the thermal performance of a double pipe heat exchanger using Al2O3-TiO2 hybrid nanofluid, Int. Commun. Heat Mass Trans. 97 (2018) 92–107.
[40]. Alok Kumar, Satyendra Singh, Experimental investigation on ThermoHydraulic performance of heat exchanger tube with solid and perforated circular disk along with twisted tape insert, Heat Trans. Eng. (2018).
[41]. Shi, X. J., et al. "Effects of geometrical parameters and Reynolds number on the heat transfer and flow characteristics of rectangular micro-channel using nano-fluid as working fluid." *Thermal Science and Engineering Progress* 15 (2020): 100456.
[42]. Gnanavel, C., R. Saravanan, and M. Chandrasekaran. "Heat transfer enhancement through nano-fluids and twisted tape insert with rectangular cut on its rib in a double pipe heat exchanger." *Materials Today: Proceedings* (2019).
[43]. Esfe, Mohammad Hemmat, Ramtin Barzegarian, and Mehdi Bahiraei. "A 3D numerical study on natural convection flow of nanofluid inside a cubical cavity equipped with porous fins using two-phase mixture model." *Advanced Powder Technology* (2020).
[44]. Ma, Yulin, Amin Shahsavar, and Pouyan Talebizadehsardari. "Two-phase mixture simulation of the effect of fin arrangement on first and second law performance of a bifurcation microchannels heatsink operated with biologically prepared water-Ag nanofluid." *International Communications in Heat and Mass Transfer* 114 (2020): 104554.
[45]. Rajabi, Amir Hossein, Davood Toghraie, and Babak Mehmandoust. "Numerical simulation of turbulent nanofluid flow in the narrow channel with a heated wall and a spherical dimple placed on it by using of single-phase and mixture-phase models." *International Communications in Heat and Mass Transfer* 108 (2019): 104316.

Amir haghighatkhah, et. al. "Numerical simulation of two-phase nanofluid flow inside a tube equipped with a vortex generator." *IOSR Journal of Mechanical and Civil Engineering (IOSR-JMCE)*, 18(1), 2021, pp. 45-55.